

# UC Davis

## UC Davis Previously Published Works

### Title

Epigenetic and genetic risk of Alzheimer disease from autopsied brains in two ethnic groups

### Permalink

<https://escholarship.org/uc/item/0v95x032>

### Journal

Acta Neuropathologica, 148(1)

### ISSN

0001-6322

### Authors

Ma, Yiyi

Reyes-Dumeyer, Dolly

Piriz, Angel

et al.

### Publication Date

2024


### DOI

10.1007/s00401-024-02778-y

Peer reviewed



# Epigenetic and genetic risk of Alzheimer disease from autopsied brains in two ethnic groups

Yiyi Ma<sup>1,2,3</sup> · Dolly Reyes-Dumeyer<sup>1,2,3</sup> · Angel Piriz<sup>1</sup> · Patricia Recio<sup>4</sup> · Diones Rivera Mejia<sup>4,5</sup> · Martin Medrano<sup>6</sup> · Rafael A. Lantigua<sup>1,7</sup> · Jean Paul G. Vonsattel<sup>1,8</sup> · Giuseppe Tosto<sup>1,2</sup> · Andrew F. Teich<sup>1,3,8</sup> · Benjamin Ciener<sup>1,3,8</sup> · Sandra Leskinen<sup>1,3,8</sup> · Sharanya Sivakumar<sup>1,3,8</sup> · Michael DeTure<sup>9</sup> · Duara Ranjan<sup>9</sup> · Dennis Dickson<sup>9</sup> · Melissa Murray<sup>9</sup> · Edward Lee<sup>10</sup> · David A. Wolk<sup>10</sup> · Lee-Way Jin<sup>11</sup> · Brittany N. Dugger<sup>11</sup> · Annie Hiniker<sup>12</sup> · Robert A. Rissman<sup>12</sup> · Richard Mayeux<sup>1,2,3</sup> · Badri N. Vardarajan<sup>1,2,3</sup> 

Received: 24 March 2024 / Revised: 1 August 2024 / Accepted: 1 August 2024  
© The Author(s) 2024

## Abstract

Genetic variants and epigenetic features both contribute to the risk of Alzheimer's disease (AD). We studied the AD association of CpG-related single nucleotide polymorphisms (CGS), which act as a hub of both the genetic and epigenetic effects, in Caribbean Hispanics (CH) and generalized the findings to Non-Hispanic Whites (NHW). First, we conducted a genome-wide, sliding-window-based association with AD, in 7,155 CH and 1,283 NHW participants. Next, using data from the dorsolateral prefrontal cortex in 179 CH brains, we tested the cis- and trans-effects of AD-associated CGS on brain DNA methylation to mRNA expression. For the genes with significant cis- and trans-effects, we investigated their enriched pathways. We identified six genetic loci in CH with CGS dosage associated with AD at genome-wide significance levels: *ADAM20* (Score = 55.19,  $P = 4.06 \times 10^{-8}$ ), the intergenic region between *VRTN* and *SYNDIGIL* (Score = -37.67,  $P = 2.25 \times 10^{-9}$ ), *SPG7* (16q24.3) (Score = 40.51,  $P = 2.23 \times 10^{-8}$ ), *PVRL2* (Score = 125.86,  $P = 1.64 \times 10^{-9}$ ), *TOMM40* (Score = -18.58,  $P = 4.61 \times 10^{-8}$ ), and *APOE* (Score = 75.12,  $P = 7.26 \times 10^{-26}$ ). CGSes in *PVRL2* and *APOE* were also significant in NHW. Except for *ADAM20*, CGSes in the other five loci were associated with CH brain methylation levels (mQTLs) and CGSes in *SPG7*, *PVRL2*, and *APOE* were also mQTLs in NHW. Except for *SYNDIGIL* ( $P = 0.08$ ), brain methylation levels in the other five loci affected downstream mRNA expression in CH ( $P < 0.05$ ), and methylation at *VRTN* and *TOMM40* were also associated with mRNA expression in NHW. Gene expression in these six loci were also regulated by CpG sites in genes that were enriched in the neuron projection and glutamatergic synapse pathways (FDR < 0.05). DNA methylation at all six loci and mRNA expression of *SYNDIGIL* and *TOMM40* were significantly associated with Braak Stage in CH. In summary, we identified six CpG-related genetic loci associated with AD in CH, harboring both genetic and epigenetic risks. However, their downstream effects on mRNA expression maybe ethnic specific and different from NHW.

**Keywords** Alzheimer's disease · Genetics · Epigenetics · Hispanics · Non-Hispanic Whites · CpG-related single nucleotide polymorphism

## Introduction

Alzheimer's disease (AD) is a chronic and progressive neurodegenerative disorder accompanied by cognitive decline that gradually worsens over years. The etiology of AD is complex involving different molecular mechanisms, which

may be the result of not only heritable genetic risks but also by factors that act on the epigenome. The advancement in identifying genetic contributions to AD has also piqued interest in epigenetic contributions. The most recent genome-wide association study (GWAS) of AD reported over 70 genetic loci for AD risk [1]. Candidate gene and genome-wide DNA methylation studies have implicated approximately 21 genetic loci with differential methylation levels associated with AD [19].

Loci identified in genetic and epigenetic studies [15] suggest a common molecular hub that captures causal risk

Richard Mayeux and Badri N. Vardarajan contributed equally to this work.

Extended author information available on the last page of the article

factors for AD. *APOE*  $\epsilon 4$  is most consistently confirmed genetic risk factor for AD and the methylation levels of the CpG island within *APOE* were found to be lower in AD brains compared to brains from healthy individuals [23]. DNA methylation occurs on the CpG dinucleotides, the single nucleotide polymorphisms altering the creation of the CpG dinucleotides are named CpG-related single nucleotide polymorphism (CGS). We previously found CGSes in the *MS4A* region have a dose-dependent effect on AD in persons who identified as non-Hispanic White (NHW) [15]. We focused our study on Caribbean Hispanics (CH) because prior studies of genetic associations of AD suggested heterogeneity across racial and ethnic groups [24].

We hypothesize that the CGS may play an important role in the risk of AD and AD pathology in Hispanics by regulating methylation and expression levels. We also investigated whether the findings in CH are unique to the population or can be generalized to other populations including non-Hispanic Whites (NHW). To test this hypothesis, we conducted a systematic analysis based on CGS in participants who identified as CH and were enrolled in Washington Heights-Inwood Columbia Aging Project (WHICAP) or the Estudio Familiar de Influencia Genética en Alzheimer (EFIGA) [21]. We used a genome-wide sliding-window approach to prioritize genetic loci comprised of CGSes associated with the risk of clinical diagnosis of AD in CH. The prioritized loci from the genome-wide analyses were followed by detailed studies to determine their function on brain DNA methylation and mRNA transcription. We analyzed both the cis- and trans-effects of the molecular mechanisms from genetics to DNA methylation and mRNA gene expression in postmortem brain tissue from CH.

## Materials and methods

### Study description

#### Cohorts included for genetic studies

We included 7,155 CH from the Washington Heights-Inwood Columbia Aging Project (WHICAP) [8] and the Estudio Familiar de Influencia Genética en Alzheimer (EFIGA) [26]. The WHICAP study is an ongoing prospective, community-based, multiethnic longitudinal study of Medicare beneficiaries 65 years and older residing in northern Manhattan (Washington Heights, Hamilton Heights, and Inwood). All the participants underwent a comprehensive examination including the assessment of general health and function, standardized physical and neurological examination, and a neuropsychological battery of tests. Follow-up visits were performed every 1.5–2 years, repeating similar examinations. Initiated in 1998, EFIGA recruited individuals of CH

ancestry including familial and sporadic AD. The individuals were recruited in New York City using local newspapers, the local CH radio station, and postings throughout the Washington Heights-Inwood neighborhood. AD was defined as any individual meeting NINCDS-ADRDA criteria for probable or possible AD [17]. The severity of dementia was rated according to the Clinical Dementia Rating [11].

We also analyzed 1,283 NHW from the Religious Order Study and the Memory & Aging Project (ROSMAP) study to investigate whether the top loci identified in the CH can be generalized to NHW. ROSMAP recruits older individuals without known dementia and their detailed information of both ante-mortem and postmortem phenotyping were collected [6]. For this study, we have included in total 1,283 NHW with whole-genome sequencing data and clinical diagnosis of AD.

#### Cohorts with brain DNA methylation and RNA sequencing (RNA-seq)

New York Brain Bank (NYBB): Tissue from the prefrontal cortex came from The NIA Alzheimer's disease family-based study (NIA-AD FBS), WHICAP, EFIGA, and NCRAD. The NIA-AD FBS included 9,682 family members, and 1,096 unrelated, nondemented elderly from different race/ethnicity groups from 1,756 families with suspected AD. NCRAD included unaffected individuals from families with a history of AD. A description of the families has been previously detailed in a report [21].

University of California, Davis Alzheimer's Disease Center (UCD ADC): With the goal to conduct research on diversity and risk of AD dementia, UCD applied an active community outreach approach to recruit the individuals from the communities of Alameda, Contra Costa, Sacramento, San Joaquin, Solano, and Yolo County. The overall percentage of CH individuals 60 years of age and older residing in these counties ranged from 7.1 to 14.3% [10]. Brain frontal cortex was dissected to measure DNA methylation and RNA sequencing.

Florida Autopsied Multi-Ethnic (FLAME) cohort: The FLAME cohort is derived from the State of Florida brain bank housed at the Mayo Clinic Florida [22]. The FLAME cohort consists of a total of 2,809 autopsied individuals with a wide range of neurodegenerative diseases, who were self-identified as Hispanic/Latino, black/African, and non-Hispanic white/European. The fixed hemi-brain (typically left hemisphere) was weighed, and the frontal cortex was cut and then placed in 10% formalin solution.

The University of Pennsylvania Integrated Neurodegenerative Disease Biobank: Patients with neurodegenerative disease are recruited into the autopsy program by the different clinical cores. The subjects selected for the autopsy were followed in the clinical centers with detailed clinical

information and most of them were also collected with biofluid, neuroimaging, and genetic data/samples. The left hemisphere and brain stem were immersed in 10% neutral buffered formalin for 2 weeks, whereas the right hemisphere was sliced coronally and frozen. Brain frontal cortex was dissected to measure DNA methylation and RNA sequencing.

University of California, San Diego Alzheimer's Disease Research Center (UCSD ADC): Postmortem frontal cortex tissue from the center's longitudinally followed cohort was used for this study. Blocks of tissue were provided from autopsy-verified cases after fixation in 10% formalin for 4 weeks. Cases were selected using detailed clinical, biomarker and demographics information collected at visits.

The Religious Order Study and the Memory & Aging Project (ROSMAP): We included 516 NHW who have measurements of both postmortem brain DNA methylation and RNA sequencing (RNA-seq) from postmortem brain tissues from the dorsolateral prefrontal cortex. The details of both datasets were described previously [6]. In brief, the grey matter from the dorsolateral prefrontal cortex (DLPFC) was dissected while still frozen. RNA was extracted for transcriptome library construction following the dUTP protocol and Illumina sequencing. The extracted DNA was processed on the Illumina Infinium HumanMethylation450 BeadChip.

An informed consent was signed by the participant and/or legal guardian of the individuals included in this study. IRB approval was approved by each institution.

## Genotype data

The genotyping in CH was conducted on the Illumina platforms (Illumina®). Standard QC metrics were applied using PLINK (v1.9) [3]. Individuals with genotype missingness  $\geq 2\%$  were removed and the SNPs were removed if their MAF  $\leq 1\%$  or Hardy–Weinberg equilibrium  $p$  value  $< 1 \times 10^{-6}$ . The genotyping data of the NHW in ROSMAP were described in detail previously [6]. Briefly, the genotyping was measured on the Affymetrix GeneChip 6.0 platform (Santa Clara, CA, USA) at the Broad Institute's Center for Genotyping or the Translational Genomics Research Institute, and the Illumina OmniQuad Express platform at Children's Hospital of Philadelphia. With PLINK, we applied the following QC filters: a genotype call rate  $> 95\%$ , MAF  $> 0.01$ , mishap test  $< 1 \times 10^{-9}$ , and a Hardy–Weinberg  $p < 0.001$ . We imputed missing genotypes using the Haplotype Reference Consortium (HRC) reference panel in both CH and NHW.

## Annotations of CpG-related SNPs (CGS)

The CpG-related single nucleotide polymorphisms (CGSes) are defined as SNPs where either the reference or the variant allele can form the CpG dinucleotides with a nearby nucleotide (Supplementary Fig. 1). With the genotype data, we calculated the dosage of CpG dinucleotides created by the multiple CGSes within each 1 Kb window and tested its association with the risk of Alzheimer's disease (AD). Prior reports have shown that the promoter sequences of approximately 1 Kb autonomously recapitulated correct DNA methylation in pluripotent cells [14]. In order to conduct a thorough investigation across the whole genome, we applied a sliding-window approach by setting the overlap between the two consecutive windows to be 500 bp, covering half of one window.

## Brain data of DNA methylation and Braak stage

The genome-wide DNA methylation profile was measured by the Infinium MethylationEPIC Kit (Illumina). We checked the control probes, sex mismatches, contamination, and genotype outliers to identify and remove samples that failed quality control. We kept CpG sites with detection  $P$  value  $< 0.01$  across all the qualified samples and masked sample-specific CpG sites with new detection  $P > 0.01$  [9]. We further removed sites reported to have cross-hybridization problems [5, 16] and polymorphic CpG sites [16, 27]. We further corrected the dye bias for all the qualified CpG probes. Finally, 179 CH samples with 675,583 autosomal probes passing QC were included in the current study. The measurement of Braak stage is described here [1].

## Brain RNA-seq data

Total RNA was extracted using Qiagen's RNeasy Mini Kit and sent to the New York Genome Center for transcriptome library construction. Sequencing was done on a NovaSeq 6000 flow cell using  $2 \times 100$  bp cycles, targeting 60 million reads per sample. All the samples included in the analysis passed QC metrics using *FastQC*. Gene counts were calculated using the *featureCounts* function. We applied *ComBat-seq* to correct batch effects. As a result, a total of 58,942 unique transcripts, including protein coding genes, pseudogenes, long non-coding and antisense RNA, passed QC metrics and exhibited non-zero expression across all participants.

## Statistical analysis

We scaled the dosage of each window to fit within a value from zero to 2 and tested the association of the scaled dosage with clinical diagnosis of AD using generalized linear mixed models (GLMMs) implemented in GMMAT [4] with adjustments for age, sex, population substructure, genomic relationship matrix (GRM), and genotyping batches. Genome-wide significance threshold was  $p < 5.0 \times 10^{-8}$ . For the mQTL analysis, brain tissue was available in 112 CH and 571 NHW participants with both genotype and brain DNA methylation data. We used generalized linear models adjusting for the age at death, sex, and technical covariates of genotyping and methylation batches, and methylation chip and position. We analyzed both the cis- and trans-effect of the DNA methylation on gene expression. For the cis-effect of DNA methylation on gene expression, we conducted a highly adaptive sum of powered score-weighted test (aSPUw) by collapsing all the available CpG sites within 100 Kb distance of the gene (from 50 Kb upstream of the transcription start site and 50 Kb downstream of the end site of the gene according to GENCODE v44 (GRCh37) annotation) with the adjustments for age, sex, and technical covariates of methylation chip ID and chip position. For the trans-effect of DNA methylation on gene expression, we used the linear mixed model to control for the random effect of methylation array, the fixed covariates of chip position on the methylation array, the batch effects, age at death, and sex. To apply a similar regression model as the clinical diagnosis of AD, we dichotomized the Braak stage variable by coding stages 5 and 6 as 1 and stages from 1 to 4 as 0. To test the effect of DNA methylation on Braak stage, we conducted the aSUPw test by collapsing CpG sites within 100 Kb distance of the gene. To test the effect of mRNA expression on Braak stage, used a logistic regression model with the binary Braak stage as the outcome and the mRNA expression level of each gene as the independent variable adjusting for age, sex, and RIN score representing the RNA integrity.

## Protein–protein interactive network and pathway analysis

There were 69 CpG sites annotated to 65 genes associated with the mRNA expression level in human brains. We investigated their network enrichment and pathway analysis using STRING (<https://string-db.org>).

## Summary statistics of African Americans

In order to replicate the results, we downloaded the summary statistics from the most recent published GWAS of AD in African Americans [20]. We extracted the CGS for the top windows identified in the CH, and tested the optimized sequence kernel association tests (SKATO) using the R ‘sumFREGAT’ package (<https://cran.r-project.org/web/packages/sumFREGAT/index.html>).

## Results

### Characteristics of the individuals providing blood and brain samples

For the analysis of clinical AD diagnosis, we included blood samples from 7,155 CH and 1,238 NHW individuals (Table 1). The population stratification of CH against the reference 1000 Genome Project is presented in Supplementary Fig. 2. The mean age of CH is 75 years, while it is 89 years for NHW individuals. 66% of both CH and NHW were women. 37% of CH and 15% NHW carried *APOE*  $\epsilon 4$  allele. There were brain samples available from 179 CH and 571 NHW individuals (Table 1). The mean age at death for CH is 80 years, while it is 88 years for NHW individuals. 57.54% of autopsied CH and 62.9% of NHW were women. Their detailed characteristics by different study site were presented in the Supplementary Table 1.

### CpG identification

Within the 7,155 CH participants, 1,857,611 1Kb windows genome-wide, with at least two CpG sites, were tested for association with the clinical diagnosis of AD. Using the Bonferroni-corrected genome-wide significance  $p$  value of  $< 5.0 \times 10^{-8}$ , we identified six genome-wide significant regions: *ADAM20* (Score = 55.19,  $P = 4.06 \times 10^{-8}$ ), the intergenic region between *VRTN* and *SYNDIG1L* (Score =  $-37.67$ ,  $P = 2.25 \times 10^{-9}$ ), *SPG7* (16q24.3) (Score = 40.51,  $P = 2.23 \times 10^{-8}$ ), *PVRL2* (Score = 125.86,  $P = 1.64 \times 10^{-9}$ ), *TOMM40* (Score =  $-18.58$ ,  $P = 4.61 \times 10^{-8}$ ), and *APOE* (Score = 75.12,  $P = 7.26 \times 10^{-26}$ ). (Fig. 1 & Table 2). The CGS windows in *PVRL2* and *APOE* were also significant in the 1,283 NHW participants from ROSMAP and 9,168 African Americans (Supplementary Table 2). However, the top CGS windows in the NHW were located in a highly linked genetic region covering *TOMM40*, *APOE*, *APOC1*, and *APOC1P1* (Fig. 1 and Supplementary Table 3). In addition, there were no sex-specific differences for the top six loci identified in the CH (Supplementary Table 4).

**Table 1** Characteristics of donors of blood and brain tissues

Blood samples				
	Hispanics (N=7155)			Whites (1238)
Age at death (y)*	75.01 (11.61)			89.59 (6.44)
Female (N) <sup>#</sup>	4760 (66.53%)			852 (66.41%)
Clinical AD diagnosis <sup>#</sup>	3961 (55.36%)			493 (38.43%)
<i>APOE</i> ε4 carriers (N) <sup>#</sup>	2674 (37.37%)			331 (15.16%)
Brain samples				
	Hispanics (N=179)			Whites (N=571)
	All (N=179)	With GWAS (N=112)	With RNA-seq (N=150)	
Age at death (y)*	80.29 (11.33)	78.52 (11.24)	81.08 (10.34)	88.32 (6.52)
Female (N) <sup>#</sup>	103 (57.54%)	64 (57.14%)	83 (55.33%)	359 (62.9%)
CERAD AD (N) <sup>a</sup>	45 (45%)	9 (27.27%)	42 (46.15%)	364 (63.75%)
NIA-REAGAN AD (N) <sup>b</sup>	136 (75.98%)	90 (80.36%)	113 (75.33%)	350 (61.30%)
Lewy Body (N) <sup>c</sup>	57 (55.34%)	39 (57.35%)	44 (38.94%)	114 (19.96%)
Braak stage (N) <sup>d</sup>	2,5,6,7,15,31,93 (0,1,2,3,4,5,6)	2,1,1,4,9,19,67	0,5,6,6,13,26,74	5,44,60,164,164,129,5

\*The mean and standard deviation of the age at death are shown

<sup>#</sup>The number and percentage of female are shown

<sup>a</sup> Individuals with CERAD definitions “Definite” and “Probable” we classified as AD pathology, while the normal controls had CERAD score defined as “Possible” and “No AD”. 79 for samples with GWAS, and 59 for samples with RNA-seq are missing CERAD scores

<sup>b</sup> NIA-REAGAN score of “High” and “Intermediate” we classified as AD patients, while the normal controls had NIA-REAGAN score of “Low” and “No AD”

<sup>c</sup> The numbers and percentages of the subjects with Lewy body pathology were presented. 49 samples in total, 44 samples with GWAS, and 37 samples with RNA-seq are missing Lewy Body pathology

Braak stage was presented by the number of subjects at stage of 0, 1, 2, 3, 4, 5, and 6

### Cis-effects of CGS on DNA methylation

We tested the cis-effects of CGS on molecular phenotypes within 100 Kb flanking the gene. The cis-effects on DNA methylation of the CpG dosage in the windows of AD are presented in Table 3 and Supplementary Fig. 3. Except for *ADAM20*, all the other five loci have significant associations between the CGSes dosage and the DNA methylation level of the CpG sites within the cis-regions: the intergenic region between *VRTN* and *SYNDIGIL* (cg16837088,  $b = -0.04$ ,  $P = 2.94 \times 10^{-3}$ ), *SPG7* (cg26536240,  $b = 0.02$ ,  $P = 5.78 \times 10^{-7}$ ), *PVRL2* (cg04406254,  $b = 0.02$ ,  $P = 2.49 \times 10^{-3}$ ), *TOMM40* (cg20051876,  $b = -0.04$ ,  $P = 0.02$ ), and *APOE* (cg20090143,  $b = -0.01$ ,  $P = 0.02$ ). In NHW, although the same CpG sites at *SPG7* ( $b = 1.75 \times 10^{-2}$ ,  $P = 6.37 \times 10^{-56}$ ) and *PVRL2* ( $b = 8.88 \times 10^{-3}$ ,  $P = 1.68 \times 10^{-4}$ ) showed statistical significance, the top significant CpG sites are different: *SPG7* (cg02244288,  $b = -0.01$ ,  $P = 2.76 \times 10^{-63}$ ) and *PVRL2* (cg02613937,  $b = -0.01$ ,  $P = 2.27 \times 10^{-6}$ ). Different CpG sites in *APOE* (cg02613937,  $b = -0.01$ ,  $P = 2.36 \times 10^{-6}$ ) showed significance in NHW. The cis-mQTLs at *ADAM20* (cg04910453,  $b = -0.02$ ,  $P = 0.05$ )

reached nominal significance ( $P \leq 0.05$ ) in NHW but not in CH.

### DNA methylation levels altering downstream cis-mRNA expression

Next, we tested the methylation sites cis-regulated by AD-associated CGSes (identified above), to determine whether these sites altered downstream mRNA expression in the brain. Since our findings revealed different methylation sites for the same gene in CH and NHW for several AD-associated loci, we conducted an aggregate analysis by collapsing all the CpG sites within the cis region of the targeted gene (Table 4). We found that except for *SYNDIGIL*, methylation levels in all the other genes significantly altered the brain RNA expression in CH ( $P \leq 0.05$ ). The significance was replicated for *VRTN* and *TOMM40* in NHW ( $P \leq 0.05$ ).

### Trans-effects of DNA methylation levels on gene expression

We tested whether the expression of the genes that harbor AD-associated CGS were influenced by genome-wide CpG

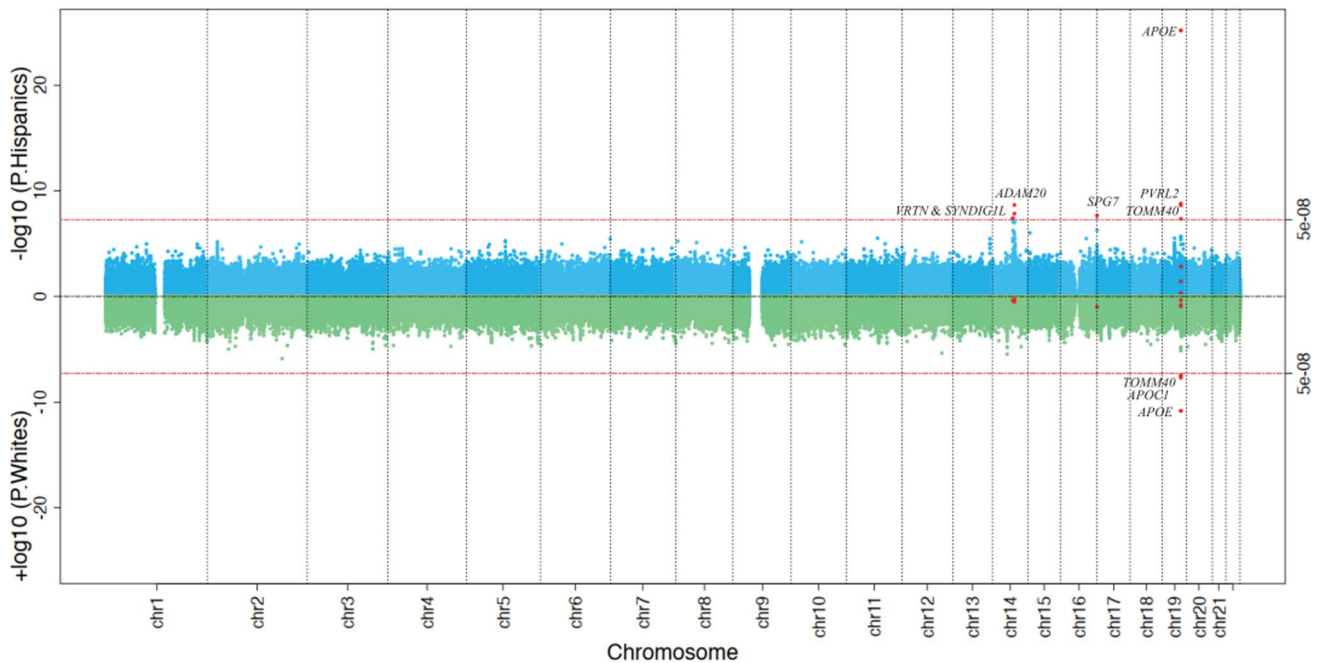


**Fig. 1** Sliding CGS window search across the genome for the risk loci of clinical diagnosis of Alzheimer disease in Hispanics and non-Hispanic Whites. The genome-wide sliding-window results for the Hispanics (upper panel in blue) and the non-Hispanic Whites (NHW) (lower panel in green) are shown in the Miami plot. Each dot repre-

sents one 1-Kb window, and X and Y axes show its genomic coordinate and  $-\log_{10}$  transformed  $P$  value. The two horizontal red lines show the Bonferroni-corrected genome-wide significance threshold ( $P \leq 5 \times 10^{-8}$ ) and those CGS windows passing the genome-wide significance threshold in either Hispanics or NHW are shown in red dots

**Table 2** Top CGS windows associated with Alzheimer's disease

Chr	Window position	Gene	Hispanics in WHICAP (N = 7155)*			Whites in ROSMAP (N = 1283)*		
			SCORE	VAR	$P$	SCORE	VAR	$P$
14	chr14:70994207–70995206	<i>ADAM20</i>	55.19	101.12	4.06E-08	1.06	1.66	0.41
14	chr14:74867207–74868206	<i>VRTN</i> and <i>SYN-DIGIL</i>	-37.67	39.70	2.25E-09	-0.20	0.11	0.56
16	chr16:89588052–89589051	<i>SPG7</i>	40.51	52.45	2.23E-08	-3.06	3.51	0.10
19	chr19:45387308–45388307	<i>PVRL2</i>	125.86	435.69	1.64E-09	11.25	5.69	2.40E-06
19	chr19:45402808–45403807	<i>TOMM40</i>	-18.58	11.56	4.61E-08	-0.13	0.009	0.17
19	chr19:45411308–45412307	<i>APOE</i>	75.12	51.03	7.26E-26	14.46	4.60	1.53E-11

\*The dosage of CpG dinucleotides created by multiple CpG-related single nucleotide polymorphisms (CGSs) of each window were scaled into the value from 0 to 2, which was analyzed for its association with Alzheimer's disease using generalized linear mixed models (GLMMs) implemented in the generalized linear mixed model association tests (GMMAT) with the adjustment of age, sex, and genotyping batches with the random effects of both kinship and genomic relationship matrix (GRM)

sites in trans. We identified 69 CpG sites across the genome that regulated gene expression of *ADAM20*, *SYNDIGIL*, *SPG7*, *PVRL2*, *TOMM40*, and *APOE* in CH at genome-wide significant levels after Bonferroni correction of the number of CpG sites included into the analysis (Supplementary Table 5). At *PVRL2* and *TOMM40*, the same CpG sites regulating the gene expression in CH also regulated the gene expression in NHW ( $P < 0.05$ ).

These 69 CpG sites that had trans-effects on the gene expressions were annotated to 65 genes. We combined these 65 genes with the target genes of *ADAM20*, *SYNDIGIL*, *SPG7*, *PVRL2*, *TOMM40*, and *APOE*, and uploaded to STRINGdb to query the significant biological pathways. The significant pathways (FDR < 0.05) are presented in Table 5, which involved neuron projection and glutamatergic synapse (FDR = 0.0189).

**Table 3** Cis-effects of CGS dosage on DNA methylation

Chr	Window position	Gene	Whites in ROSMAP (N=571)										Correlation between White top and Hispanic top CpG sites						
			Hispanics in WHICAP (N=112)					Whites in ROSMAP (N=571)					Hispanics		Whites				
			CpG sites (N)	P threshold	CpG	Position	BETA	STDERR	P	Same CpG site in Hispanics	CpG site with minimum P in Whites	Position	BETA	STDERR	P	R	R		
14	chr14:70994207-70995206	ADAM20	7	7.14E-03	cg04910453	71,051,130	0.01	0.01	0.37	-0.02	0.01	0.05	cg04910453	71,051,130	-0.02	0.01	0.05	1	1
14	chr14:74867207-74868206	VRTN and SYN-DIGTL	95	5.26E-04	cg16837088	74,742,111	-0.04	0.01	2.94E-03	NA	NA	NA	cg13074788	74,720,261	-0.01	6.42E-03	0.06	0.17	NA
16	chr16:89588052-89589051	SPG7	186	2.69E-04	cg26536240	89,509,760	0.02	0.004	5.78E-07	1.75E-02	9.74E-04	6.37E-04	cg02244288	89,573,955	-0.01	7.49E-04	2.76E-63	-0.48	-0.3
19	chr19:45387308-45388307	PVRL2	67	7.46E-04	cg04406254	45,407,945	0.02	0.007	2.49E-03	8.88E-03	2.34E-03	1.68E-04	cg02613937	45,395,297	-0.01	2.87E-03	2.27E-06	-0.12	-0.14
19	chr19:45402808-45403807	TOMM40	61	8.20E-04	cg20051876	45,407,860	-0.04	0.02	0.02	NA	NA	NA	NA	NA	NA	NA	NA	NA	NA
19	chr19:45411308-45412307	APOE	69	7.25E-04	cg20090143	45,452,003	-0.01	0.004	0.02	-9.05E-04	1.23E-03	0.46	cg02613937	45,395,297	-0.01	2.42E-03	2.36E-06	-0.31	0.1

BETA, STDERR, and P represent the regression coefficient and its corresponding standard error, and P values of the generalized linear mixed regression model where the dosage of CpG dinucleotides created by multiple CpG-related single nucleotide polymorphisms (CGSs) of each window were exposure variables and DNA methylation level of each included CpG sites were outcome variable with the adjustment of age, sex, batches of genotyping and methylation, methylation array position with the random effect of methylation array

Abbreviations: AD, Alzheimer’s disease

R represents the correlation coefficient between two CpG sites



**Table 4** Cis-effects of DNA methylation on gene expression

Chr	Gene	Hispanics in WHICAP (N=150)					Whites in ROSMAP (N=516)				
		SPUw1		aSPUw		P values range	SPUw1		aSPUw		P values range
		T	P	T	P		T	P	T	P	
14	<i>ADAM20</i>	-7.25	0.09	0.01	0.03	[0.012, 0.09]	4.04E-16	0.16	0.10	0.25	[0.1, 0.55]
14	<i>VRTN</i>	-63.76	0.05	0.003	8.00E-03	[0.003, 0.046]	9.99E-16	0	0	9.99E-04	[0, 0.000999]
14	<i>SYNDIGIL</i>	-26.52	0.40	0.03	0.08	[0.03, 0.40]	1.09E-14	0.25	0.03	0.08	[0.03, 0.25]
16	<i>SPG7</i>	-129.93	0.002	0	9.99E-04	[0, 0.005]	5.01E-12	0.47	0.27	0.61	[0.27, 0.62]
19	<i>PVRL2</i>	-75.43	0.002	0	9.99E-04	[0, 0.002]	-4.57E-13	0.19	0.12	0.25	[0.12, 0.25]
19	<i>TOMM40</i>	17.37	0.38	0.003	0.01	[0.003, 0.38]	8.57E-13	0.02	0.02	0.03	[0.02, 0.03]
19	<i>APOE</i>	-83.13	0.001	0	9.99E-04	[0, 0.001]	-2.07E-11	0.96	0.04	0.12	[0.04, 0.97]

<sup>#</sup>We have conducted a highly adaptive sum of powered score-weighted test to collapse all the available CpG sites within 100 Kb distance to the gene and analyze their associations on the gene expression. SPUw1 provides the direction of the score, indicating the effect direction of DNA methylation on gene expression, where aSPUw test simply combines the results of multiple SPUw tests by taking the minimum P values. The model is Gaussian for the continuous gene expression values

\*T and P represent the statistic and its corresponding P values

SPUw1 sum of powered score-weighted 1 test, aSPUw adaptive sum of powered score-weighted tests

**Table 5** Pathway analysis of the trans-effects of DNA methylation on gene expression

Category	Term ID	Term description	Observed gene count	Background gene count	Strength	False discovery rate
GO Component	GO:0030054	Cell junction	19	2115	0.43	0.0189
GO Component	GO:0030424	Axon	11	651	0.71	0.0189
GO Component	GO:0043005	Neuron projection	16	1391	0.54	0.0189
GO Component	GO:0098978	Glutamatergic synapse	8	334	0.86	0.0189
Monarch	EFO:0004612	High density lipoprotein cholesterol measurement	14	740	0.76	0.0015
Monarch	EFO:0004732	Lipoprotein measurement	17	1426	0.56	0.017
Monarch	EFO:0004614	Apolipoprotein A 1 measurement	9	396	0.84	0.0275
Monarch	EFO:0005105	Lipid or lipoprotein measurement	22	2526	0.42	0.0345
Monarch	EFO:0004529	Lipid measurement	21	2400	0.42	0.0365
Monarch	EFO:0004582	Liver enzyme measurement	14	1124	0.58	0.0365
Monarch	EFO:0004747	Protein measurement	36	5856	0.27	0.0365
TISSUES	BTO:0001484	Nervous system	42	6016	0.33	4.03e-05
TISSUES	BTO:0000227	Central nervous system	39	5825	0.31	0.00044
TISSUES	BTO:0000142	Brain	38	5733	0.3	0.00067
TISSUES	BTO:0000282	Head	39	6642	0.25	0.0081
COMPARTMENTS	GOCC:0030054	Cell junction	15	1053	0.64	0.0033
COMPARTMENTS	GOCC:0045202	Synapse	9	493	0.74	0.0426
UniProt Keywords	KW-0025	Alternative splicing	52	10,313	0.18	0.0024

## Effect of brain DNA methylation and mRNA expression on postmortem Braak stage

We collapsed all the CpG sites within the cis region of the targeted gene and all six genes have significant effects on Braak stage (Table 6). The downstream mRNA expression of *ADAM20*, *SYNDIGIL*, and *TOMM40* also have significant effects on Braak stage.

## Discussion

We have conducted the first multi-omics investigation of CpG-related SNPs (CGS) in brain tissue from a group of individuals of CH ancestry, which confer both genetic and epigenetic effects among individuals. Our study is one of the largest genome-wide association studies with the focus

**Table 6** Effect of DNA methylation and mRNA expression on Braak stage\*

Gene	DNA methylation <sup>#</sup>		mRNA expression <sup>§</sup>		
	SPUw1_T	aSPUw_P	BETA	STDERR	P
<i>ADAM20</i>	-3.06	1.60E-02	5.21E-03	3.03E-03	8.52E-02
<i>VRTN</i>	-35.73	9.99E-04	-7.65E-02	1.41E-01	5.86E-01
<i>SYNDIGIL</i>	-35.73	9.99E-04	1.92E-02	8.24E-03	1.98E-02
<i>SPG7</i>	-57.63	3.00E-03	-3.02E-05	2.15E-04	8.88E-01
<i>PVRL2</i>	-50.44	9.99E-04	-5.06E-04	8.33E-04	5.44E-01
<i>TOMM40</i>	-24.59	9.99E-04	-3.38E-03	1.32E-03	1.06E-02
<i>APOE</i>	-40.51	9.99E-04	2.84E-05	5.21E-05	5.86E-01

\*Braak stage was transformed into a binary variable, where scores 5 and 6 are coded as 1 and scores from 1 to 4 are coded as 0

<sup>#</sup>We have conducted a highly adaptive sum of powered score-weighted test to collapse all the available CpG sites within 100 Kb distance to the gene and analyze their associations on the gene expression. SPUw1 provides the direction of the score, indicating the effect direction of DNA methylation on gene expression, where aSPUw test simply combines the results of multiple SPUw tests by taking the minimum P values. The model is binomial for the binary variable of Braak stage

<sup>§</sup>We have conducted a logistic regression model with the binary Braak stage as the outcome variable and the mRNA expression level of each gene as the exposure variable adjusting for the covariate of age, sex, and RIN score representing the RNA integrity. The regression coefficient, standard error, and P value are represented

SPUw1\_T sum of powered score-weighted 1 test statistic estimate, aSPUw\_P P value of the adaptive sum of powered score-weighted tests

on CGS in this ethnic group. We then assessed the effect cascade from the AD-associated CGSes to brain methylation levels to brain mRNA expression levels.

This study was unique in terms of its use of human brain tissues for AD in CH. In addition, the current study provided robust results which survived the most stringent Bonferroni correction for multiple testing. Results from this study emphasize the importance of studying minority groups. Many of the top CGS windows found in NHW were also significant in CH; however, many of the top CGS windows identified in CH were not replicated in NHW.

We identified six genome-wide significant windows in or near *ADAM20*, *VRTN*, *SYNDIGIL*, *SPG7*, *PVRL2*, *TOMM40*, and *APOE*, where the dosage of the CpG dinucleotides (created by the including CGSes) were associated with the risk of clinical diagnosis of AD. In *SPG7*, the AD-associated CGS window is associated with increased cis-DNA methylation levels in the frontal cortex, which in turn reduced downstream mRNA expression. We validated the *SPG7* genetic and epigenetic alterations in NHW, but did not find an effect on mRNA expression. Similarly, for *PVRL2* and *APOE*, we identified AD-associated CGSes which in turn regulated methylation levels in both CH and NHW brains. However, the epigenetic modifications had muted effect on downstream gene expression. At *PVRL2*, both the cis-effects and trans-effects were statistically significant.

*SPG7* gene encodes paraplegin, a component of the m-AAA protease, an ATP-dependent proteolytic complex of the mitochondrial inner membrane that degrades misfolded

proteins and regulates ribosome assembly. Our finding of its significant effects of its association with AD was consistent with the previous report that the DNA methylation level at *SPG7* was associated with Braak neurofibrillary stages [13]. *PVRL2* (a.k.a. *NECTIN2*) encodes a gene within the nectin subfamily of immunoglobulin-like adhesion molecules that participate in Ca<sup>2+</sup>-independent cell-cell adhesion. It is upstream of *TOMM40* and *APOE* and is located within the highly linked genetic cluster of *TOMM40-APOE-APOC2*. *PVRL2* had both cis- and trans-effects between DNA methylation and mRNA gene expression. The CpG island within *APOE* was reported to have lower DNA methylation levels in AD patients compared to controls in human postmortem brains [7, 25], which is more profound in glial cells [25]. Lee et al [12] reported a negative correlation between *APOE* total RNA and DNA methylation levels at the CpG island within *APOE* in human postmortem frontal lobes, and this negative correlation is stronger in controls compared to AD patients. *SYNDIGIL* (also known as *TMEM90A* or *CAPUCIN*) encodes synapse differentiation-induced gene 1 like. In rodents, memory and motor deficits caused by 1,2-Diacetylbenzene via alteration of the mRNA expression of *Syndig11* [18] can be improved by prolactin.

Although this investigation is currently one of the the largest with CH brain DNA methylation data, it does have limitations of potential bias by grey vs. white matter composition driven by different protocols used by different brain banks. In addition, the fact that multiple sites contribute to the brain samples may also bring variations into the findings.

Since the brain samples from different sites were measured in different methylation batches, we included batch (but not the contributing site) as a covariate in the regression model to remove the colinear bias. In addition, we only investigated DNA methylation patterns in the human postmortem brain. The brain is the most relevant tissue to study AD, and DNA methylation is tissue specific which presents a challenge to generalize the findings from human brains to peripheral blood. In addition, our cross-sectional study design does not account for change in DNA methylation due to normal aging, although we adjusted for age in the regression model. Generally, the higher dosage of CGS in a window should lead to higher methylation levels in that window, the effect direction of the CGS dosage on a single CpG site that is not included within the window are unknown. In such cases, it is reasonable to have the negative association between the CGS dosage of the window and methylation level of CpG site within the 100 Kb distance to the annotated gene, such as *VRTN* and *SYNDIGIL*, *TOMM40*, and *APOE*.

We report six statistically robust genetic loci covering seven genes that act as a hub for both the genetic and epigenetic effects on clinical diagnosis of AD in CH: *ADAM20*, the intergenic region between *VRTN* and *SYNDIGIL*, *SPG7*, *PVRL2*, *TOMM40*, and *APOE*. *PVRL2* and *APOE* were also genetically significant in NHW. Except *ADAM20*, all the other loci have significant mQTL effects in CH, and *SPG7*, *PVRL2*, *APOE* also have significant mQTL in NHW. The DNA methylation levels of all seven genes except for *SYNDIGIL* have significant associations with its mRNA gene expression levels in CH brains, while only *VRTN* and *TOMM40* also showed significant associations on mRNA expression levels in NHW brains. Except for *VRTN*, the mRNA gene expression levels of all the other six genes have significant trans-effects from DNA methylation levels of the CpG sites in CH, while only *PVRL2* and *TOMM40* also showed trans-effects in NHW. *PVRL2* had both significant cis- and trans-effects from the genetics to epigenetics and then to the mRNA gene expression. The genes for the trans-effects are enriched in the pathways of neuron projection and glutamatergic synapse. *SPG7* and *APOE* had significant cis-effects, while *SYNDIGIL* has significant trans-effects. In addition, their downstream effects on mRNA expression maybe ethnic specific and different from NHW. Finally, the findings in the Hispanics cannot be fully generalized to the non-Hispanic Whites, which might be because of the genetic differences between diverse ancestries.

**Supplementary Information** The online version contains supplementary material available at <https://doi.org/10.1007/s00401-024-02778-y>.

**Acknowledgements** We thank all the investigators for this study. We thank Dr. David Bennett for releasing ROSMAP datasets publicly. Data collection and sharing for this project was supported by (WHICAP, R01 AG072474, R01 AG066107) funded by the National Institute

on Aging (NIA) and by the National Center for Advancing Translational Sciences, National Institutes of Health, through Grant Number UL1TR001873. Data collection and analysis for this project was supported by the Genetic Studies of Alzheimer disease in Caribbean Hispanics (EFIGA) funded by the National Institute on Aging (NIA) and by the National Institutes of Health (NIH) (R01 AG067501 and U01 AG066752). The project was partially funded by the National Institute on Aging (NIA) of the National Institutes of Health (NIH) under Award Numbers R01AG062517, and P30AG072972, P30AG062429, NIA (P30 AG062677, P01 AG003949), Florida Department of Health, Ed and Ethel Moore Alzheimer Disease Research Program (20A22, 8AZ06), NIH P30AG072979, P01AG066597 and U19AG062418.

**Data availability** We will put the summary data in Zenodo. The raw DNA methylation data will be shared through NIAGADS, AD knowledge portal, and upon request via the WHICAP/EFIGA data sharing forms.

**Open Access** This article is licensed under a Creative Commons Attribution-NonCommercial-NoDerivatives 4.0 International License, which permits any non-commercial use, sharing, distribution and reproduction in any medium or format, as long as you give appropriate credit to the original author(s) and the source, provide a link to the Creative Commons licence, and indicate if you modified the licensed material. You do not have permission under this licence to share adapted material derived from this article or parts of it. The images or other third party material in this article are included in the article's Creative Commons licence, unless indicated otherwise in a credit line to the material. If material is not included in the article's Creative Commons licence and your intended use is not permitted by statutory regulation or exceeds the permitted use, you will need to obtain permission directly from the copyright holder. To view a copy of this licence, visit <http://creativecommons.org/licenses/by-nc-nd/4.0/>.


## References

1. Bellenguez C, Küçükali F, Jansen IE, Kleindam L, Moreno-Grau S, Amin N, Naj AC et al (2022) New insights into the genetic etiology of Alzheimer's disease and related dementias. *Nat Genet* 54(4):412–436. <https://doi.org/10.1038/s41588-022-01024-z>
2. Braak H, Alafuzoff I, Arzberger T, Kretschmar H, Del Tredici K (2006) Staging of Alzheimer disease-associated neurofibrillary pathology using paraffin sections and immunocytochemistry. *Acta Neuropathol* 112:389–404. <https://doi.org/10.1007/s00401-006-0127-z>
3. Chang CC, Chow CC, Tellier LC, Vattikuti S, Purcell SM, Lee JJ (2015) Second-generation PLINK: rising to the challenge of larger and richer datasets. *Gigascience* 4:7. <https://doi.org/10.1186/s13742-015-0047-8>
4. Chen H, Wang C, Conomos MP, Stilp AM, Li Z, Sofer T et al (2016) Control for population structure and relatedness for binary traits in genetic association studies via logistic mixed models. *Am J Hum Genet* 98:653–666. <https://doi.org/10.1016/j.ajhg.2016.02.012>
5. Chen YA, Lemire M, Choufani S, Butcher DT, Grafodatskaya D, Zanke BW et al (2013) Discovery of cross-reactive probes and polymorphic CpGs in the Illumina Infinium HumanMethylation450 microarray. *Epigenetics* 8:203–209. <https://doi.org/10.4161/epi.23470>
6. De Jager PL, Ma Y, McCabe C, Xu J, Vardarajan BN, Felsky D et al (2018) A multi-omic atlas of the human frontal cortex for aging and Alzheimer's disease research. *Sci Data* 5:180142. <https://doi.org/10.1038/sdata.2018.142>

7. Foraker J, Millard SP, Leong L, Thomson Z, Chen S, Keene CD et al (2015) The APOE gene is differentially methylated in Alzheimer's disease. *J Alzheimers Dis* 48:745–755. <https://doi.org/10.3233/JAD-143060>
8. Gu Y, Honig LS, Kang MS, Bahl A, Sanchez D, Reyes-Dumeyer D et al (2024) Risk of Alzheimer's disease is associated with longitudinal changes in plasma biomarkers in the multi-ethnic Washington Heights-Hamilton Heights-Inwood Columbia Aging Project (WHICAP) cohort. *Alzheimers Dement*. <https://doi.org/10.1002/alz.13652>
9. Heiss JA, Just AC (2019) Improved filtering of DNA methylation microarray data by detection p values and its impact on downstream analyses. *Clin Epigenet* 11:15. <https://doi.org/10.1186/s13148-019-0615-3>
10. Hinton L, Carter K, Reed BR, Beckett L, Lara E, DeCarli C et al (2010) Recruitment of a community-based cohort for research on diversity and risk of dementia. *Alzheimer Dis Assoc Disord* 24:234–241. <https://doi.org/10.1097/WAD.0b013e3181c1ee01>
11. Hughes CP, Berg L, Danziger WL, Coben LA, Martin RL (1982) A new clinical scale for the staging of dementia. *Br J Psychiatry* 140:566–572. <https://doi.org/10.1192/bjp.140.6.566>
12. Lee EG, Tulloch J, Chen S, Leong L, Saxton AD, Kraemer B et al (2020) Redefining transcriptional regulation of the APOE gene and its association with Alzheimer's disease. *PLoS ONE* 15:e0227667. <https://doi.org/10.1371/journal.pone.0227667>
13. Li QS, Sun Y, Wang T (2020) Epigenome-wide association study of Alzheimer's disease replicates 22 differentially methylated positions and 30 differentially methylated regions. *Clin Epigenet* 12:149. <https://doi.org/10.1186/s13148-020-00944-z>
14. Lienert F, Wirbelauer C, Som I, Dean A, Mohn F, Schubeler D (2011) Identification of genetic elements that autonomously determine DNA methylation states. *Nat Genet* 43:1091–1097. <https://doi.org/10.1038/ng.946>
15. Ma Y, Jun GR, Chung J, Zhang X, Kunkle BW, Naj AC et al (2019) CpG-related SNPs in the MS4A region have a dose-dependent effect on risk of late-onset Alzheimer disease. *Aging Cell* 18:e12964. <https://doi.org/10.1111/acer.12964>
16. McCartney DL, Walker RM, Morris SW, McIntosh AM, Porteous DJ, Evans KL (2016) Identification of polymorphic and off-target probe binding sites on the Illumina Infinium MethylationEPIC BeadChip. *Genom Data* 9:22–24. <https://doi.org/10.1016/j.gdata.2016.05.012>
17. McKhann GM, Knopman DS, Chertkow H, Hyman BT, Jack CR Jr., Kawas CH et al (2011) The diagnosis of dementia due to Alzheimer's disease: recommendations from the National Institute on Aging-Alzheimer's Association workgroups on diagnostic guidelines for Alzheimer's disease. *Alzheimer's & Dementia J Alzheimer's Assoc* 7(3):263–269. <https://doi.org/10.1016/j.jalz.2011.03.005>
18. Nguyen HD, Jo WH, Hoang NHM, Kim MS (2022) In silico identification of the potential molecular mechanisms involved in protective effects of prolactin on motor and memory deficits induced by 1,2-Diacetylbenzene in young and old rats. *Neurotoxicology* 93:45–59. <https://doi.org/10.1016/j.neuro.2022.09.002>
19. Nikolac Perkovic M, Videtic Paska A, Konjevod M, Kouter K, Svob Strac D, Nedic Erjavec G et al (2021) Epigenetics of Alzheimer's Disease. *Biomolecules*. <https://doi.org/10.3390/biom11020195>
20. Ray NR, Kunkle BW, Hamilton-Nelson K, Kurup JT, Rajabli F, Cosacak MI et al (2023) Extended genome-wide association study employing the African Genome Resources Panel identifies novel susceptibility loci for Alzheimer's Disease in individuals of African ancestry. *MedRxiv*. <https://doi.org/10.1101/2023.08.29.23294774>
21. Reyes-Dumeyer D, Faber K, Vardarajan B, Goate A, Renton A, Chao M et al (2022) The national institute on aging late-onset Alzheimer's disease family based study: a resource for genetic discovery. *Alzheimers Dement* 18:1889–1897. <https://doi.org/10.1002/alz.12514>
22. Santos OA, Pedraza O, Lucas JA, Duara R, Greig-Custo MT, Hanna Al-Shaikh FS et al (2019) Ethnoracial differences in Alzheimer's disease from the FLorida autopsied multi-ethnic (FLAME) cohort. *Alzheimers Dement* 15:635–643. <https://doi.org/10.1016/j.jalz.2018.12.013>
23. Shao Y, Shaw M, Todd K, Khrestian M, D'Aleo G, Barnard PJ et al (2018) DNA methylation of TOMM40-APOE-APOC2 in Alzheimer's disease. *J Hum Genet* 63:459–471. <https://doi.org/10.1038/s10038-017-0393-8>
24. Tosto G, Reitz C (2013) Genome-wide association studies in Alzheimer's disease: a review. *Curr Neurol Neurosci Rep* 13:381. <https://doi.org/10.1007/s11910-013-0381-0>
25. Tulloch J, Leong L, Thomson Z, Chen S, Lee EG, Keene CD et al (2018) Glia-specific APOE epigenetic changes in the Alzheimer's disease brain. *Brain Res* 1698:179–186. <https://doi.org/10.1016/j.brainres.2018.08.006>
26. Vardarajan BN, Faber KM, Bird TD, Bennett DA, Rosenberg R, Boeve BF et al (2014) Age-specific incidence rates for dementia and Alzheimer disease in NIA-LOAD/NCRAD and FIGA families: National Institute on Aging Genetics Initiative for Late-Onset Alzheimer Disease/National Cell Repository for Alzheimer Disease (NIA-LOAD/NCRAD) and Estudio Familiar de Influencia Genetica en Alzheimer (FIGA). *JAMA Neurol* 71:315–323. <https://doi.org/10.1001/jamaneurol.2013.5570>
27. Zhou W, Laird PW, Shen H (2017) Comprehensive characterization, annotation and innovative use of Infinium DNA methylation BeadChip probes. *Nucleic Acids Res* 45:e22. <https://doi.org/10.1093/nar/gkw967>

**Publisher's Note** Springer Nature remains neutral with regard to jurisdictional claims in published maps and institutional affiliations.

## Authors and Affiliations

Yiyi Ma<sup>1,2,3</sup> · Dolly Reyes-Dumeyer<sup>1,2,3</sup> · Angel Piriz<sup>1</sup> · Patricia Recio<sup>4</sup> · Diones Rivera Mejia<sup>4,5</sup> · Martin Medrano<sup>6</sup> · Rafael A. Lantigua<sup>1,7</sup> · Jean Paul G. Vonsattel<sup>1,8</sup> · Giuseppe Tosto<sup>1,2</sup> · Andrew F. Teich<sup>1,3,8</sup> · Benjamin Ciener<sup>1,3,8</sup> · Sandra Leskinen<sup>1,3,8</sup> · Sharanya Sivakumar<sup>1,3,8</sup> · Michael DeTure<sup>9</sup> · Duara Ranjan<sup>9</sup> · Dennis Dickson<sup>9</sup> · Melissa Murray<sup>9</sup> · Edward Lee<sup>10</sup> · David A. Wolk<sup>10</sup> · Lee-Way Jin<sup>11</sup> · Brittany N. Dugger<sup>11</sup> · Annie Hiniker<sup>12</sup> · Robert A. Rissman<sup>12</sup> · Richard Mayeux<sup>1,2,3</sup> · Badri N. Vardarajan<sup>1,2,3</sup> 

✉ Richard Mayeux  
rpm2@cumc.columbia.edu

✉ Badri N. Vardarajan  
bnv2103@cumc.columbia.edu

<sup>1</sup> Taub Institute for Research on Alzheimer's Disease and the Aging Brain, Vagelos College of Physicians and Surgeons, Columbia University, New York, NY, USA

<sup>2</sup> G.H. Sergievsky Center, Vagelos College of Physicians and Surgeons, Columbia University, New York, NY, USA

<sup>3</sup> Department of Neurology, Vagelos College of Physicians and Surgeons, Columbia University, The New York Presbyterian Hospital, 630 West 168th street, New York, NY 10032, USA

<sup>4</sup> CEDIMAT, Santo Domingo, Dominican Republic

<sup>5</sup> Universidad Pedro Henríquez Urena, Santo Domingo, Dominican Republic

<sup>6</sup> Pontificia Universidad Católica Madre y Maestra (PUCMM), Santiago, Dominican Republic

<sup>7</sup> Department of Medicine, Vagelos College of Physicians and Surgeons, Columbia University, The New York Presbyterian Hospital, New York, NY, USA

<sup>8</sup> Department of Pathology and Cell Biology, Vagelos College of Physicians and Surgeons, Columbia University, New York, NY, USA

<sup>9</sup> Department of Neuroscience, Mayo Clinic Florida, Jacksonville, FL, USA

<sup>10</sup> Department of Neurology and Penn Alzheimer's Disease Research Center, Perelman School of Medicine, University of Pennsylvania, Philadelphia, PA, USA

<sup>11</sup> Department of Pathology and Laboratory Medicine, School of Medicine, University of California Davis, Sacramento, CA 95817, USA

<sup>12</sup> Keck School of Medicine of the University of Southern California, Los Angeles, CA, USA